^{12}C emission from ^{114}Ba and nuclear properties

D. N. Poenaru,[1,2,3] W. Greiner,[1] and E. Hourani[2]
[1]*Institut für Theoretische Physik der Universität, Frankfurt am Main, Postfach 111932, D-60054 Frankfurt am Main, Germany*
[2]*Institut de Physique Nucléaire, F-91406 Orsay Cedex, France*
[3]*Institute of Atomic Physics, P.O. Box MG-6, RO-76900 Bucharest, Romania*
(Received 11 October 1994)

We investigate the influence of nuclear masses, radii, and interaction potentials on ^{12}C radioactivity of ^{114}Ba—the best representative of a new island of cluster emitters leading to daughter nuclei around the doubly magic ^{100}Sn. Three different models are considered: one derived by Blendowske, Fliessbach, and Walliser (BFW) from the many-body theory of α decay, as well as our analytical (ASAF) and numerical (NuSAF) superasymmetric fission models. A Q value larger by 1 MeV or an ASAF potential barrier reduced by 3% are producing a half-life shorter by 2 orders of magnitude. A similar effect can be obtained within BFW and NuSAF by a decrease of the action integral with less than 10% and 5%, respectively. By increasing the radius constant within ASAF or BFW models by 10%, the half-life becomes shorter by 3 orders of magnitude.

PACS number(s): 23.70.+j, 27.60.+j

I. INTRODUCTION

In 1984 two of us predicted the ^{12}C radioactivity of ^{114}Ba (see [1, 2]), the ^{16}O radioactivity of neutron-deficient Ce isotopes, and a whole island of cluster emitters ending with daughters in the neighborhood of ^{100}Sn. At that time, the importance of the magic numbers of protons and neutrons of the daughter, and the proton-richness of the parent nuclei was stressed. Also mentioned, was the difficulty of performing reliable calculations due to the lack of mass measurements in this region of nuclei very far from the line of beta stability. Nevertheless, in 1988 we did new calculations with different mass estimations [3] and presented the results in comprehensive tables which appeared in 1989 as preprints (larger preliminary versions of the paper [4]).

The ^{12}C emission from ^{114}Ba has been very clearly mentioned by Price in his review article [5] among experiments worth doing. We have presented the new island of cluster emission, stressing the unusually high branching ratio possible with respect to α decay, at many international conferences [St. Petersburg, 1989, Predeal Summer Schools in 1990 and 1992 (NATO Advanced Study Institute), Louvaine-la-Neuve, 1991, Bernkastel-Kues, 1992, Mainz, 1993]. The detection of cluster radioactivity in this region of nuclei [6] has been held as one of the interesting experiments justifying the funding of a new accelerator [7].

The most probable emitted cluster from a proton-rich nucleus (like ^{114}Ba) is ^{12}C and from a beta-stable or neutron-rich nucleus (like ^{224}Ra), ^{14}C, due to a substantial difference in the corresponding Q values (about 11 and 4 MeV, respectively).

In spite of the good agreement of our predictions with the half-lives measured since 1984 in the trans-radium region (daughters around ^{208}Pb), and of the agreement of calculations of other models (for example the best representative BFW [8] of the preformed cluster models) with our calculations in this new region of nuclei, the preliminary results of recently performed measurements [9, 10] seems to indicate an emission rate higher than expected.

The ^{114}Ba parent nucleus is very far from stability—almost on the proton drip line. It was not produced until very recently, and therefore none of its properties, including the decay modes (β^+, α, etc.), have been experimentally determined. In Darmstadt [9] ^{114}Ba was produced by (^{58}Ni, ^{58}Ni) reaction followed by mass separation. The study of its decay properties is in progress. A deeper discussion of the physics we can learn from the experimental results would be possible when the masses, the decay energies, and the partial and total half-lives are determined with a high accuracy. At present, we can investigate some of the nuclear properties able to accommodate an increased emission probability. In this paper the discussion will be focused on the following physical quantities: mass values, nuclear radii, and potential barriers.

The (measurable) decay constant λ is expressed as a product of three (model-dependent) quantities:

$$\lambda = \nu S P \tag{1}$$

frequency of assaults ($\nu = 2E_v/h$) or the zero-point vibration energy E_v (where h is the Planck constant), preformation probability of the emitted cluster into the parent nucleus (S), and the (external) barrier penetrability (P). As we have shown, by presenting various theoretical models [11] developed since 1985, the frequency of assaults is usually considered to be in the range 10^{20}–10^{22} /sec. One can take it either as a constant or allow for a small variation which is not very significant for the present discussion. We expect that the preformation probability would not be extremely sensitive to the variation of the above mentioned nuclear properties, hence the main contribution would come from the barrier

penetrability. Nevertheless, we shall calculate all three quantities.

II. A NUMERICAL SUPERASYMMETRIC FISSION MODEL

We have used a first variant of the numerical superasymmetric fission (NuSAF) model in 1979 to describe α decay as a fission process. In a second approach, the reduced mass has been replaced by the Werner-Wheeler inertia [12]. The one-dimensional two-center parametrization of the nuclear shape has been considered. Recently we developed [13] a new method to find the optimum fission trajectory in a three-dimensional deformation space by solving a nonlinear system of differential equations with partial derivatives.

In the NuSAF model the nuclear energy, replacing the Myers-Swiatecki's liquid drop model surface energy, is given by the double folded Yukawa-plus-exponential (Y+E) potential [14] energy

$$E_Y = -\frac{c_s}{8\pi^2 r_0^2 a^4}\int_{V_n}\int\left(\frac{r_{12}}{a}-2\right)\frac{\exp(-r_{12}/a)}{r_{12}/a}d^3r_1 d^3r_2, \tag{2}$$

where $r_{12} = |\mathbf{r}_1 - \mathbf{r}_2|$, $a = 0.68$ fm is the diffusivity parameter, and $c_s = a_s(1-\kappa I^2)$, $a_s = 21.13$ MeV is the surface energy constant, $\kappa = 2.3$ is the surface asymmetry constant, $I = (N-Z)/A$, and $r_0 = 1.16$ fm is the nuclear radius constant.

By taking into account the difference between the charge densities of the two fragments, this energy can be expressed [15] as a sum of two self-energies and one interaction energy between them:

$$\begin{aligned}E_Y = &-\frac{c_{s1}}{8\pi^2 r_0^2 a^4}\int_{V_1} d^3r_1\int_{V_1}\left(\frac{r_{12}}{a}-2\right)\frac{e^{-r_{12}/a}}{r_{12}/a}d^3r_2\\ &-\frac{2\sqrt{c_{s1}c_{s2}}}{8\pi^2 r_0^2 a^4}\int_{V_1} d^3r_1\int_{V_2}\left(\frac{r_{12}}{a}-2\right)\frac{e^{-r_{12}/a}}{r_{12}/a}d^3r_2\\ &-\frac{c_{s2}}{8\pi^2 r_0^2 a^4}\int_{V_2} d^3r_1\int_{V_2}\left(\frac{r_{12}}{a}-2\right)\frac{e^{-r_{12}/a}}{r_{12}/a}d^3r_2.\end{aligned} \tag{3}$$

For overlapping fragments with axial symmetry, the sixfold integrals can be reduced to three-dimensional ones which are calculated numerically [15] by Gauss-Legendre quadrature. A spherical compound nucleus with a radius $R_0 = r_0 A^{1/3}$ gives

$$E_Y^0 = c_{s0}A^{2/3}\{1-3x^2+(1+1/x)[2+3x(1+x)]e^{-2/x}\} \tag{4}$$

in which $x = a/R_0$.

Similar to the (Y+E) term, one has a Coulomb energy:

$$\begin{aligned}E_C = &\frac{\rho_{1e}^2}{2}\int_{V_1} d^3r_1\int_{V_1}\frac{d^3r_2}{r_{12}}+\frac{\rho_{2e}^2}{2}\int_{V2} d^3r_1\int_{V2}\frac{d^3r_2}{r_{12}}\\ &+\rho_{1e}\rho_{2e}\int_{V1} d^3r_1\int_{V2}\frac{d^3r_2}{r_{12}},\end{aligned} \tag{5}$$

where the first two terms belong to individual fragments and the third one represents their interaction. The charge densities of the compound nucleus and of the two fragments are denoted by ρ_{0e}, ρ_{1e}, and ρ_{2e}, respectively. The Coulomb energy of a spherical nucleus with mass number A is given by

$$E_C^0 = \frac{3e^2Z^2}{5r_0A^{1/3}}. \tag{6}$$

The total deformation energy is the sum of the Y+E, Coulomb, and the volume terms:

$$E = E_Y + E_C + E_V. \tag{7}$$

When the fragments are separated, i.e., the distance, R, between the centers of the two fragments is larger than the touching-point configuration value $R_t = R_1 + R_2$ (where R_1 and R_2 are the radii of the fragments), analytical relationships are available:

$$E_C = \frac{Z_1Z_2e^2}{R}, \tag{8}$$

$$\begin{aligned}E_Y = -4\left(\frac{a}{r_0}\right)\sqrt{c_{s1}c_{s2}}\Bigg[&g_1g_2\left(4+\frac{R}{a}\right)\\ &-g_2f_1-g_1f_2\Bigg]\frac{e^{-R/a}}{R/a},\end{aligned} \tag{9}$$

where

$$f_k = \left(\frac{R_k}{a}\right)^2\sinh\frac{R_k}{a}, \tag{10}$$

$$g_k = \frac{R_k}{a}\cosh\frac{R_k}{a}-\sinh\frac{R_k}{a}, \quad (k=1,2). \tag{11}$$

The Werner-Wheeler approximation allows to obtain analytical relationships for nuclear inertia if one uses the two-center shape parametrization.

The preformation, S, and the penetrability of the external barrier, P, are given by $S = \exp(-K_{ov})$, $P = \exp(-K_s)$. They are calculated within the Wentzel-Kramers-Brillouin (WKB) approximation where in the one-dimensional case, the action integrals, K_{ov} (for overlapping fragments) and K_s (for separated fragments), are expressed as

$$K_{ov,s} = \frac{2}{\hbar}\int_{R_a,R_t}^{R_t,R_b}[2B(R)E(R)]^{(1/2)}dR, \tag{12}$$

in which B is nuclear inertia equal to the reduced mass $\mu = mA_eA_d/A$ for separated fragments, m is the nucleon mass, and $E(R)$ is the interaction energy of the two fragments separated by the distance R between centers from which the Q value has been subtracted. R_a and R_b are the turning points of the WKB integral.

The zero-point vibration energy can be estimated from the stiffness of the potential barrier and the effective mass parameter:

$$E_v = \frac{\hbar}{R_t - R_i}\sqrt{\frac{E_b}{2\mu}} = \frac{4.5536}{R_t - R_i}\sqrt{\frac{AE_b}{A_e A_d}};\ E_b = E(R_t) - Q \tag{13}$$

where R_t and $R_i = R_0 - R_2$ are the separation distances at the touching- and initial-point, respectively. In this equation the energies are expressed in MeV and the distances in fm. For α decay and ^{14}C radioactivity of different nuclei, one obtains values in the range 1.6–2.3 MeV and 1.0–1.35 MeV, respectively, and minima at the magic number of neutrons for the daughter nucleus. The zero-point vibration energies of various models are in the range 1–8 MeV.

The inertia tensor, $\{B_{ij}\}$, depends on the arbitrarily chosen set of shape coordinates $\{q_i\}$. The Werner-Wheeler approximation to irrotational flow motion within a hydrodynamical model can be used in a wide range of mass asymmetry of the final fragments, and allows to obtain analytical results. One has to stress the importance of taking into account a correction term, B^c_{ij}, due to the center of mass motion [12]. The components of the inertia tensor are calculated with the following equations:

$$B_{ij} = \pi\sigma \int_{z_{\min}}^{z_{\max}} \rho_s^2 (X_i X_j + \tfrac{1}{2} Y_i Y_j) dz + B^c_{ij}, \tag{14}$$

$$B^c_{ij} = -(\pi^2\sigma/V) \int_{z_{\min}}^{z_{\max}} \rho_s^2 X_i dz \int_{z_{\min}}^{z_{\max}} \rho_s^2 X_j dz, \tag{15}$$

where $\rho_s = \rho_s(z)$ is the nuclear surface equation in cylindrical coordinates, with $z_{\min}, z_{\max}$ intercepts on the z axis. V is the volume of the system, assumed to be conserved, $\sigma = 3m/(4\pi r_0^3)$ is the mass density, m is the nucleon mass. Functions X_i and Y_i are found as a sum of two terms for the left (l) and right (r) side of the shape:

$$X_{il} = -\rho_s^{-2} \frac{\partial}{\partial q_i} \int_{z_{\min}}^{z} \rho_s^2 dz, \tag{16}$$

$$X_{ir} = \rho_s^{-2} \frac{\partial}{\partial q_i} \int_{z}^{z_{\max}} \rho_s^2 dz,$$

$$Y_{ir(l)} = -\frac{\rho_s}{2} \frac{\partial}{\partial z} X_{ir(l)}. \tag{17}$$

For another set of deformation parameters $\{p\}$ describing the same shape,

$$B_{kl}(p) = \sum B_{ij}(q) \frac{\partial q_i}{\partial p_k} \frac{\partial q_j}{\partial p_l}. \tag{18}$$

The contributions of the left- (B_1) and right- (B_2) sides to inertia are given by

$$4r_0^3 B_i(R)/3m = (z_i')^2 V_i/\pi + (-1)^i 2 z_i' R_i R_i' (R_i + D_i)^2 + (R_i R_i')^2 [2R_i^2/H_i - 4.5R_i - 3.5D_i + 6R_i \ln(2R_i/H_i)] \tag{19}$$

and the correction B_c, added to the sum $B_1 + B_2$ is determined by

$$4r_0^3 B_c(R)/3m = -(3/4R_0^3)C^2; \quad C = C_1 + C_2, \tag{20}$$

$$C_i = (z_i')^2 V_i/\pi + (-1)^i R_i R_i' (R_i + D_i)^2; \quad (i = 1, 2), \tag{21}$$

where $D_1 = z_s - z_1$, $D_2 = z_2 - z_s$, $H_i = R_i - D_i$, z_s is the position of intersection plane of the spheres, and z_i are the geometrical centers of the spheres. The superscript prime denotes derivative with respect to R. The above equations become very simple for an origin in the center of the first sphere ($z_1' = 0$). When the origin is in the separation plane and in the center of mass, z_1' is replaced by $-D_1'$ and $(z_1 - z_c)'$, respectively. In all cases $z_2' = z_1' + R'$. Here $z_c - z_1$ is the distance of the center of mass relative to the center of the first sphere.

For a three-dimensional parametrization of nuclear shape (two spheres smoothly joined by a surface generated when a circle is rotated around the axis of symmetry) [16] the components of the nuclear inertia tensor have been calculated numerically. We performed calculations for α decay, ^{28}Mg radioactivity, and cold fission (with the light fragment ^{100}Zr) of ^{234}U—the first nucleus for which all three decay modes have been experimentally detected. In the absence of the smoothed neck (the one-dimensional parametrization of two intersected spheres with cusp), we obtained $K_{ov} = 7.1\%$, 35.2%, and 62.5%, respectively (for the three decay modes), from the total value of $K = K_{ov} + K_s$. In the three-dimensional case, as a result of the minimization along the optimum dynamical path, K_{ov}/K has been reduced to $(K_{ov}/K)_{opt} = 5.9\%$, 32.9%, and 55%, respectively. A decrease of the potential barrier by multiplication of $[E(R) - Q]$ with a factor $f^2 < 1$ (due to deformations or increased nuclear radii) will lead to an f times lower value of the action integral $K = fK_0$.

In this way, the best fit [rms of $\log_{10} T(s)$ values of 0.51, comparable to 0.49 of Blendowske-Fliessbach-Walliser (BFW) [17] and to 0.47 of the analytical superasymmetric fission (ASAF) models] to 14 even-even cluster radioactivities measured until now [18, 19] is obtained when $f = 0.8985 \simeq 0.9$. The experimental and theoretical results are plotted in Fig. 1 for ten of these measured events versus the mass number of the parent nucleus. For ^{234}U and ^{238}Pu three different cluster emissions have been experimentally determined [5]; we selected only one for each parent in Fig. 1 in order to simplify the presentation. A value of f which is lower for the NuSAF than for the BFW model is understandable from the comparison of the corresponding potentials in

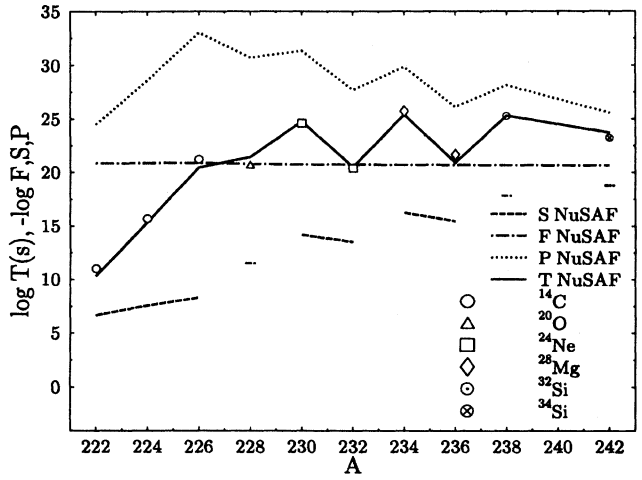

FIG. 1. Half-lives T of ten even-even nuclei against cluster decays and the corresponding three model-dependent quantities (< 1): F (preexponential factor), S (preformation probability), and P (penetrability of the external barrier) calculated within the numerical superasymmetric fission model. The experimentally determined half-lives are also shown. Decimal logarithms (log) are given.

the next section (Fig. 3).

From Fig. 1 one can see that the variation of the preexponential factor $F = \ln 2/\nu$ can be neglected in comparison with that of the penetrability P. Also the preformation probability S is very much dependent on the mass number of the emitted cluster, but it is less sensitive to that of the parent nucleus.

By assuming that the same optimum value $K/K_0 = 0.9$ will be also obtained in the new island of cluster emitters, the half-life will be shorter by two orders of magnitude than that estimated within ASAF or BFW. A similar reduction has been obtained by Buck *et al.* [20].

III. VARIOUS INTERACTION POTENTIALS, NUCLEAR RADII, AND Q VALUES

Our ASAF model is based on the liquid-drop model developed in 1966-67 by Myers and Swiatecki [21], which is known to overestimate the fission barrier height E_b^0. This was the reason why we had introduced a correction energy E_c, playing also the role of a phenomenological shell correction (in the spirit of Strutinsky's method). Up to now we have only considered a dependence of this quantity on the mass number of the emitted cluster and the Q value. It seems that this quantity should also depend on the daughter nucleus, which would be reasonable in view of an important contribution of the Coulomb forces to the height of the barrier.

A higher value of E_c produces a lower barrier height and an increased barrier penetrability. For example, we have initially at Q=20.75 MeV, with a lowering of the potential barrier by 5.5% (E_c=1.66 MeV), a half-life of $T = 10^{6.57}$ s. By increasing E_c by a factor 2 (meaning that the barrier height is decreased by 11%), the half-life becomes shorter by about 4 orders of magnitude ($T = 10^{2.64}$ s).

An indication for a need of a lower potential barrier to describe the new region of nuclei can be deduced from Fig. 2. In this figure we compare the rms deviations from the experimental results

$$\mathrm{rms} = \left\{ \left[\sum_{i=1}^{n} (\log_{10} T_i - \log_{10} T_{\mathrm{exp}})^2 \right] / (n-1) \right\}^{1/2} \tag{22}$$

in three groups of even-even alpha emitters: three isotopes of Te, 13 isotopes of Po, and 124 parents (including Te and Po isotopes) with atomic numbers from $Z = 52$ to $Z = 102$ and mass numbers $A = 106$–256. The minimum deviation from the experimental results is obtained for $E_c/E_c^0 = 1$ (or $f = 1$ within BFW) in the large collectivity of data, but at about $E_c/E_c^0 = 1.4$ (or $f = 0.98$ within BFW) for the lightest parents leading to daughter nuclei not far from ^{100}Sn [22]. A similar trend is not observed in case of NuSAF, which gives almost the same

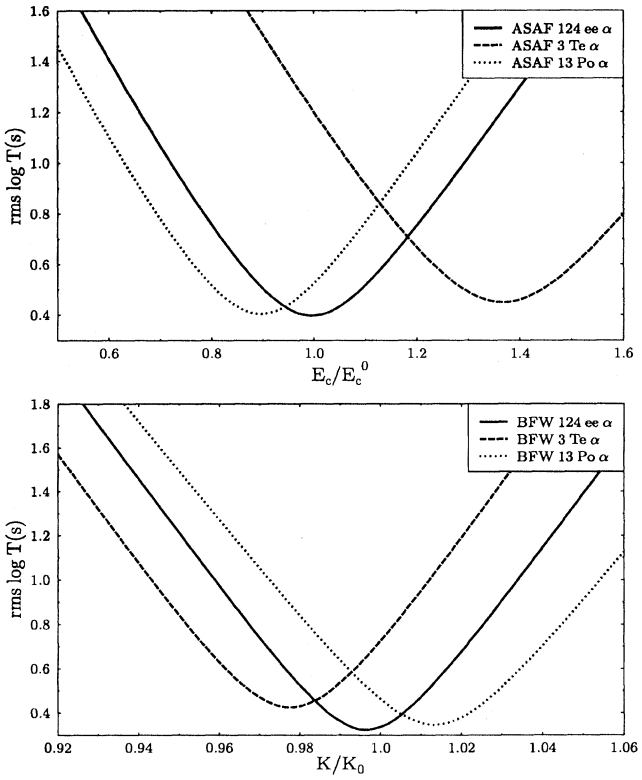

FIG. 2. Deviations of half-lives for α decay calculated within ASAF (upper part) and BFW (lower part) from the experimental ones vs the correction energy E_c/E_c^0 and the action integral K/K_0, respectively. Three groups of even-even parent nuclei are considered: three Te isotopes, 13 Po isotopes, and 124 various nuclei with atomic numbers in the range 52 – 102. Decimal logarithms (log) are given.

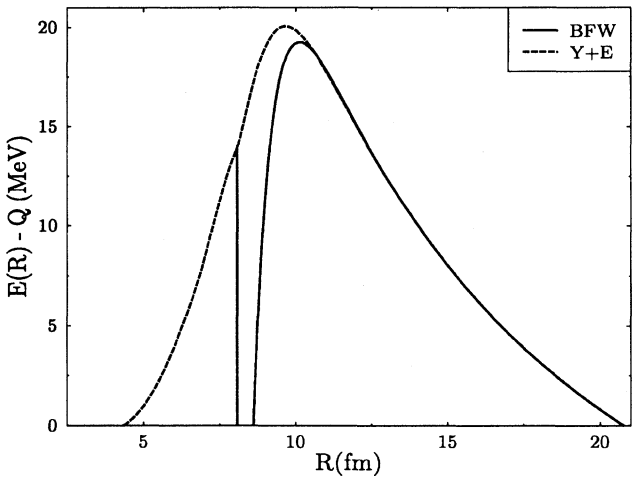

FIG. 3. Potential barrier $E(R)-Q$ for ^{12}C radioactivity of ^{114}Ba (Q = 20.79 MeV) within the BFW and NuSAF models. The vertical line corresponds to the touching point separation distance.

optimum value f =0.94 for all groups.

As we have discussed above, the larger f for NuSAF compared to BFW comes from the higher potential barrier of Y+E [14]. Both potentials Y+E and that used by BFW [23] have been successful for heavy-ion elastic scattering. A typical example may be seen in Fig. 3 for the ^{12}C emission from ^{114}Ba. The touching point radii are similar, 8.04 fm in Y+E and 7.95 fm in BFW, but $E(R_t) = -50.1$ MeV and $E > Q$ beginning with R =8.6 fm for BFW. In fact, from a similar figure [11] in which many other potentials used to study cluster emission have been compared, BFW presented the lowest and thinnest barrier.

When we get the experimental Q and T we can fix the E_c/E_c^0 or f (and consequently the potential barrier) in this new region of parent nuclei (see Fig. 4). The relative emission rate of various emitted clusters will not be essentially affected by this tuning; ^{12}C will remain the most probable emitted cluster from ^{114}Ba, and the Ba isotope with A=114 will remain the parent with highest emission rate (except for ^{112}Ba which is expected to decay by two-proton emission).

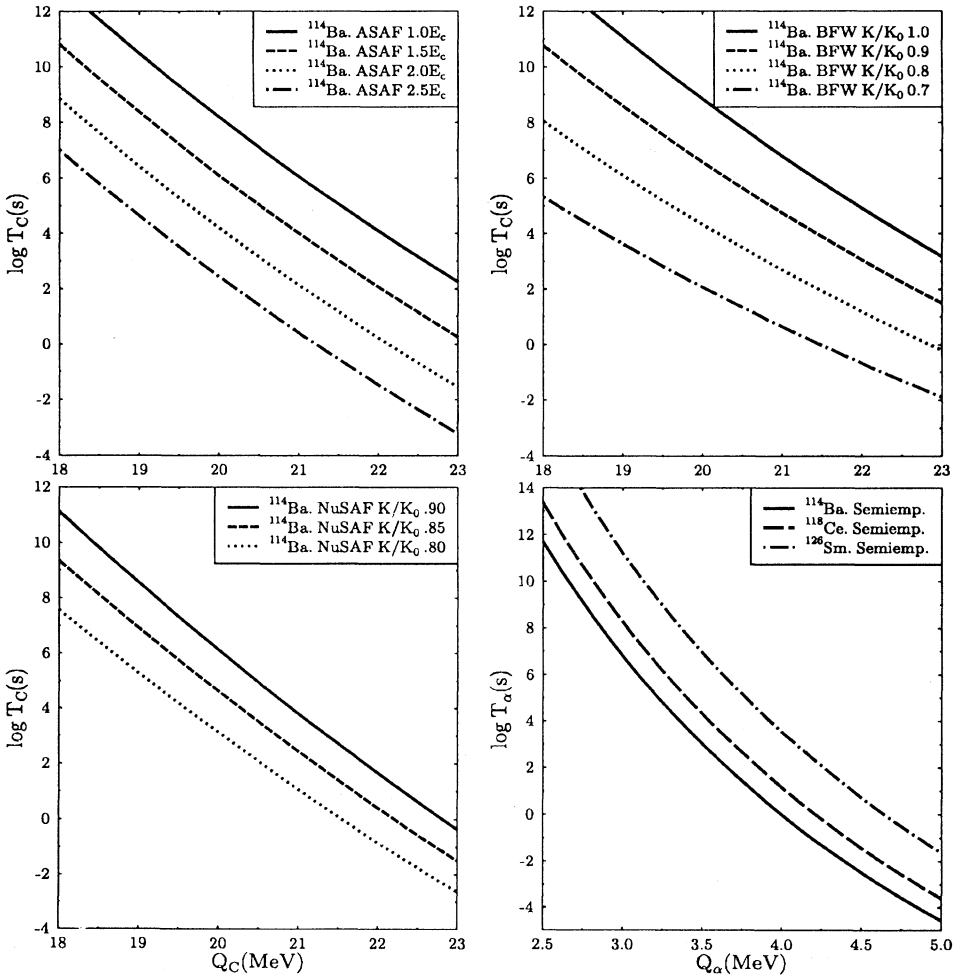

FIG. 4. Variation with Q value and correction energy E_c/E_c^0 or action integral K/K_0 of the ^{114}Ba partial half-life for ^{12}C radioactivity (plots at the top and bottom left) and variation with Q_α of ^{114}Ba, ^{118}Ce, ^{126}Sm partial half-life for α decay (bottom right). When the experimental data on Q and T will be available one can determine an eventual need for a lower potential barrier within ASAF, BFW, or NuSAF. In a similar way can be tested the predictive power of our semiempirical formula for α decay. Decimal logarithms (log) are given.

TABLE I. Q values for ^{12}C decay of ^{114}Ba according to different mass estimations.

Mass code	11	9	8	12	3
Q (MeV)	20.75	20.20	19.97	18.34	18.16

A lower potential barrier could also account for the unexplained high cross section of the low-energy (subbarrier) fusion. On the other hand, a multidimensional tunneling approach would be desirable in cluster radioactivity of ^{114}Ba.

A possible contribution from the most probable ^{12}C radioactivity of ^{112}Ba (producing the daughter ^{100}Sn) which would have an increased Q value by about 2 MeV and hence, a shorter half-life by about 4 orders of magnitude, should be ruled out for at least two reasons. The mass (and on-line chemical separation) performed in the experiment [9] to obtain ^{114}Ba was free from contamination with A=112 isotope, and according to all mass estimations, the ^{112}Ba is unstable toward two proton emission.

Apart from the emitted particles, the nuclei implicated in the β, α, and ^{12}C decays of ^{114}Ba are ^{102}Sn, ^{110}Xe, ^{114}Cs, and ^{114}Ba. From these only Cs, Xe, and Sn are mentioned in the new mass table [24] as being directly measured (Cs) or having the mass determined from systematics (Xe,Sn). By taking only a few (more optimistic or with good reproduction of experimental data) of the more than 15 available mass values, both for the parent and daughter nuclei from the same table, one obtains the Q values given in Table I for the ^{12}C emission from ^{114}Ba, where the mass codes conventionally adopted by us are: 11-Pearson *et al.* [25]; 9-Möller and Nix [26]; 8-Möller *et al.* [27]; 12-Liran and Zeldes [28]; 3-Jänecke and Masson [29].

For α decay, we have estimated the half-lives given in Table II using our semiempirical formula. In Fig. 4 (bottom right) we show results for other Q values and parent nuclei. Of course, similar figures can be drawn for the other ^{12}C, ^{16}O, and ^{28}Si emissions we mentioned long ago.

Let us consider the following [9] (preliminary) measured values for ^{12}C emission from ^{114}Ba: Q=18.1 MeV, $\log_{10} T(s)$ =4.23, and $\log_{10} T_\alpha(s)$ >2.7. It follows from Fig. 4 that ^{12}C decay data will be reproduced by ASAF with E_c/E_c^0 =3.253, by BFW with K/K_0=0.666, and by NuSAF with K/K_0 =0.7117. Also our semiempirical relationship for α decay leads to $Q_\alpha \leq$3.549 MeV.

An increased effective radius (for example due to nuclear deformation) will also produce a similar effect of lowering the potential barrier. The best fit of Te isotopes data is obtained if the nuclear radii are increased by 10% within ASAF (equivalent to E_c/E_c^0 =1.4) or by 5% within BFW (or f =0.98).

TABLE II. Half-lives and Q values for α decay of ^{114}Ba according to different mass tables.

Mass code	8	9	12	11	3
Q_α (MeV)	3.035	3.125	3.155	3.465	3.475
$\log_{10} T(s)$	6.52	5.78	5.54	3.26	3.19

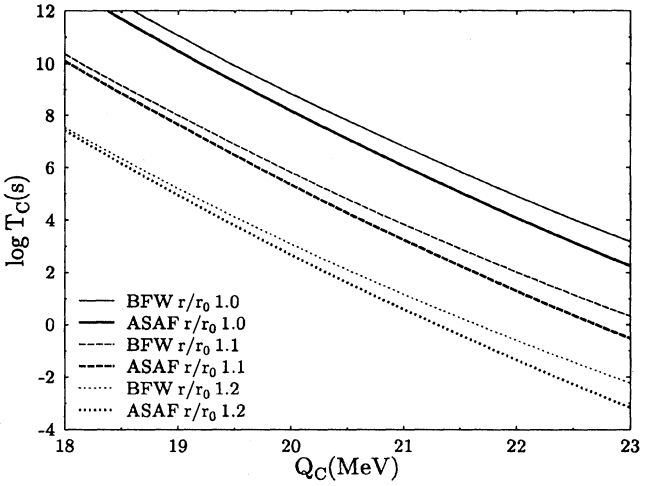

FIG. 5. The sensitivity of the half-life for ^{12}C decay of ^{114}Ba to the variation of nuclear radii and Q value within the BFW and ASAF models. Decimal logarithms (log) are given.

The sensitivity of the half-life for ^{12}C decay of ^{114}Ba to the variation of nuclear radii and Q value within BFW and ASAF models can be estimated from Fig. 5. Around Q = 20 MeV a nuclear radius constant larger by 10% lowers the fission barrier and leads to a half-life shorter by 3 orders of magnitude.

IV. CONCLUSIONS

The measurement of ^{114}Ba partial half-lives and Q values against ^{12}C- and α decay will allow to determine the nuclear properties (masses, radii, interaction potentials) in this region of nuclei far from stability, by comparison with the corresponding calculations. We have analyzed the sensitivity of two fission models (ASAF, NuSAF) and of one model (BFW), derived from traditional many-body theory of alpha decay, to the variation of these quantities. For light emitted clusters (He, C, O, etc.) the internal part of the barrier is much thinner than the external one. Consequently the main variation of the half-life is predominantly due to the (external) barrier penetrability (and to a less extent to preformation probability).

Around Q=20 MeV a Q value larger by 1 MeV or an ASAF correction energy increased by 50% (reduction by 3% of the barrier height) produce a half-life shorter by two orders of magnitude. A similar effect can be obtained within BFW and NuSAF by a decrease of the action integral (which may be due to a lower potential barrier) with less than 10% and 5%, respectively. By increasing the radius constant (which could simulate a deformation for example) within ASAF or BFW models by 10%, the

half-life decreases by 3 orders of magnitude.

Both ASAF and BFW models show similar results for α decay and cluster radioactivities in various regions of the nuclear chart. The Y+E potential used by NuSAF leads to a somewhat different behavior. If we adopt the same optimum value $K/K_0 = 0.9$ in the new island of cluster emitters, the half-life is by 2 orders of magnitude shorter than that estimated within ASAF or BFW, pointing out the importance of the chosen nuclear potential.

We are sure that this interesting problem of nuclear physics, which we raised in 1984, will continue to be a subject of future experimental and theoretical investigations.

ACKNOWLEDGMENTS

We had stimulating discussions with P. B. Price, E. Roeckl, R. Bonetti, and A. Guglielmetti. We are grateful to D. Lunney for critical reading of the manuscript. This work was supported by the Bundesministerium für Forschung und Technologie, the Deutsche Forschungsgemeinschaft, the KfK Karlsruhe, Le Ministere de l'Enseignement Superieur et de la Recherche, Paris, and the Institute of Atomic Physics. One of us (D.N.P.) has received a donation of computer and copying equipment from the Soros Foundation for an Open Society.

[1] W. Greiner, M. Ivaşcu, D. N. Poenaru, and A. Săndulescu, in *Treatise on Heavy Ion Science*, edited by D. A. Bromley (Plenum, New York, 1989), Vol. 8, p. 641.
[2] D. N. Poenaru, W. Greiner, and R. Gherghescu, Phys. Rev. C **47**, 2030 (1993).
[3] P. E. Haustein, At. Data Nucl. Data Tables **39**, 185 (1988).
[4] D. N. Poenaru, D. Schnabel, W. Greiner, D. Mazilu, and R. Gherghescu, At. Data Nucl. Data Tables **48**, 231 (1991).
[5] P. B. Price, Annu. Rev. Nucl. Part. Sci. **39**, 19 (1989).
[6] D. N. Poenaru and W. Greiner, in *Proceedings of the 2nd International Conference on Radioactive Nuclear Beams, Louvain-la-Neuve, 1991*, edited by T. Delbar (IOP, Bristol, 1992), p. 203.
[7] P. Dalpiaz, "The ADRIA proposal," Istituto Nationale di Fisica Nucleare, Report LNL–INFN 58/92, 1992.
[8] R. Blendowske, T. Fliessbach, and H. Walliser, Nucl. Phys. **A464**, 75 (1987).
[9] A. Guglielmetti *et al.*, Nucl. Phys. A (to be published).
[10] Yu. Ts. Oganessian, V. L. Mikheev, and S. P. Tretyakova, private communication.
[11] D. N. Poenaru and W. Greiner, in *Clustering Phenomena in Atoms and Nuclei*, edited by M. Brenner, T. Lönnroth, and B. Malik (Springer, Heidelberg, 1992), p. 235.
[12] D. N. Poenaru, J. A. Maruhn, W. Greiner, M. Ivaşcu, D. Mazilu, and I. Ivaşcu, Z. Phys. A **333**, 291 (1989).
[13] M. Mirea, D. N. Poenaru, and W. Greiner, Z. Phys. A **349**, 39 (1994).
[14] W. Scheid and W. Greiner, Z. Phys. A **226**, 364 (1969); H. J. Krappe, J. R. Nix, and A. J. Sierk, Phys. Rev. C **20**, 992 (1979).
[15] D. N. Poenaru, M. Ivaşcu, and D. Mazilu, Comput. Phys. Commun. **19**, 205 (1980).
[16] M. Mirea, D. N. Poenaru, and W. Greiner, Nuovo Cimento A **105**, 571 (1992).
[17] R. Blendowske, T. Fliessbach, and H. Walliser, chapter in Nuclear Decay Modes (IOP, Bristol, in press).
[18] E. Hourani, chapter in Nuclear Decay Modes [17].
[19] R. Bonetti and A. Guglielmetti, chapter in Nuclear Decay Modes [17].
[20] B. Buck, A. C. Merchant, S. M. Perez, and P. Tripe, J. Phys. G **20**, 351 (1994).
[21] W. D. Myers and W. J. Swiatecki, Nucl. Phys. **A81**, 1 (1966).
[22] E. Roeckl, Rep. Prog. Phys. **55**, 1661 (1992).
[23] P. R. Christensen and A. Winther, Phys. Lett. **65B**, 19 (1976).
[24] G. Audi and A. H. Wapstra, Nucl. Phys. **A565**, 1 (1993).
[25] Y. Aboussir, J. M. Pearson, A. K. Dutta, and F. Tondeur, Nucl. Phys. **A549**, 155 (1992).
[26] P. Möller and J. R. Nix, At. Data Nucl. Data Tables **39**, 213 (1988).
[27] P. Möller, W. D. Myers, W. J. Swiatecki, and J. Treiner, At. Data Nucl. Data Tables **39**, 225 (1988).
[28] S. Liran and N. Zeldes, At. Data Nucl. Data Tables **17**, 431 (1976).
[29] J. Jänecke and P. J. Masson, At. Data Nucl. Data Tables **39**, 265 (1988).